J. Fluid Mech. (1997), *vol.* 332, *pp.* 141–156
Copyright © 1997 Cambridge University Press

Turbulent dispersion with broken reflectional symmetry

By MICHAEL S. BORGAS,[1] THOMAS K. FLESCH[2] AND BRIAN L. SAWFORD[1]

[1] CSIRO Division of Atmospheric Research, Aspendale, Victoria 3195, Australia

[2] University of Alberta, Edmonton, Canada

(Received 21 April 1995 and in revised form 2 September 1996)

We consider dispersion in axisymmetric turbulence which lacks reflectional symmetry. A stochastic equation for the Lagrangian evolution of the velocity of a fluid particle, which is appropriate for infinite Reynolds number turbulence, is used to model the dispersion. Such equations are now common as Lagrangian dispersion models for atmospheric transport problems, but are only strictly well founded for isotropic homogeneous turbulence. It is the minimalist variation from this state of affairs that is considered here. Axisymmetry is the most highly symmetric turbulence that can be suitably analysed by these techniques, spherical symmetry being equivalent to full isotropy in the class of models considered. This simple relaxation of full symmetry leads to oscillations of the Lagrangian velocity autocorrelation, oscillatory growth of the dispersion, significant reduction of dispersion for fixed turbulence kinetic energy and dissipation rate, spiralling fluid-particle trajectories, and tracer fluxes orthogonal to gradients (skew diffusion). The mean fluid-particle angular momentum is an important parameter.

1. Introduction

Taylor (1921) was the first person to study turbulent dispersion using Lagrangian concepts (i.e. marked fluid particles with negligible molecular motion of transported quantities) and he obtained a relation between mean-square dispersion from a point and the velocity autocorrelation. Further, for ideal turbulent flows (homogeneous, isotropic and stationary), when a simple exponential decorrelation of the velocity is perhaps appropriate, he obtained a functional expression for the dispersion with a single undetermined constant (time scale). Subsequently, this functional form has been largely accepted in practical work and the unknown constant has been identified with a universal inertial-range constant for velocity increments (Inoue 1952; Obukhov 1959; Thomson 1987; Borgas & Sawford 1991). In modern parlance, the Lagrangian evolution of a fluid particle velocity is well approximated by a Markov process, i.e. particle accelerations at different times are uncorrelated. Sawford (1991) shows how this asymptotic state arises for large Reynolds number (i.e. when viscous effects are negligible). Even when intermittency effects are explicitly taken into consideration (Borgas & Sawford 1994*a*), there is little change to Taylor's original picture. Recent work (Borgas & Sawford 1996) also shows the utility of Markovian Lagrangian models for describing measured passive-scalar dispersion in grid-generated wind-tunnel turbulence.

When the flow is not isotropic or homogeneous, it is possible to have an enormous

https://doi.org/10.1017/S002211209600393X Published online by Cambridge University Press

range of complex behaviour. Such behaviour is poorly understood in the Lagrangian context except for the simplest idealized flow described above. Thus as a precursor to considering realistic turbulent flows, for example, modelling the atmospheric boundary layer, we shall study the simplest non-trivial non-isotropic flow: homogeneity and as much symmetry as is possible will be maintained. Turbulent flows which lack reflectional symmetry (Batchelor 1953), but are otherwise isotropic, are marginally more complex than the fully isotropic case. However, when flows are axisymmetric and lack reflectional symmetry we shall find gross changes from the behaviour (exponential autocorrelations) described above.

Flows lacking reflectional symmetry are often characterized by a pseudo-scalar called *helicity*, which is simply the average value of the scalar product of velocity and vorticity (Moffatt & Tsinober 1992). However, the flows we examine with one-particle Lagrangian methods cannot be related explicitly to this Eulerian characteristic. Implicitly, it is clear that there is some connection between the flows that we consider and flows that have helicity. There are important transport effects associated with flows with non-zero helicity: Kraichnan (1977) argues that helicity augments turbulent dispersion, Cieszelski (1994) argues that helicity is 'anti-diffusive' and Moffatt (1983) describes effects such as skew diffusion (transport orthogonal to gradients). Here we shall examine turbulent dispersion from the Lagrangian viewpoint (i.e. following Taylor 1921) and have something to say about the dispersive power as well as about skew diffusion.

The turbulence we consider belongs most properly to the *axisymmetric* class of flows because it is necessary to discriminate a special spatial direction in order to construct a non-trivial solution. In fact, many physical situations that lack reflexional symmetry are most simply idealized as axisymmetric turbulence: for example, a rotating turbulent fluid mass with the axis of rotation as the special spatial direction (Zeman 1994), or with the axis aligned with a magnetic field in a turbulent flow of electrically conducting fluid (Moffatt 1983), or with the axis running along a wind tunnel with an array of right (or left) handed propellers acting as a grid (Kholmyansky *et al.* 1991). Atmospheric flows where helicity is considered important are, of course, tornadoes, and also boundary-layer roll vortices (Etling 1985; Angell, Pack & Dickson 1967), but these are circumstances where the mean flow is itself complex and has a dominant helical component and the explicit role of the underlying turbulence is less of a factor in the behaviour.

We thus focus on flows with trivial mean-velocity fields and with homogeneous turbulence characteristics, but where the turbulent eddies have some preferred sense of rotation. The question to be asked is what are the implications for dispersion and how is the broken reflection symmetry to be quantified.

The aspects of dispersion that we are capable of describing here are simply mean-field characteristics, i.e. the spatial distribution of the mean concentration and mean fluxes. Probability distributions of passive scalar (at a point say) are not determined by the one-particle dispersion, even when molecular diffusivity effects are neglected. The broader picture of dispersion encompassed by full probability distributions, even just second moments like the scalar variance, or intermittency concepts (Chatwin & Sullivan 1989), require more sophisticated models than are presented here. We simply assess the implication of broken reflection for fluid particle dispersion and its role in mean-field passive-scalar dynamics.

Below we describe the stochastic model equations which are appropriate for describing the (high Reynolds number) flow as postulated. We specialize to axisymmetric turbulence and use Thomson's (1987) considerations to obtain a general

https://doi.org/10.1017/S002211209600393X Published online by Cambridge University Press

form of this equation which has unspecified constants, reflecting a non-unique formulation. The potential non-uniqueness of the stochastic equations is a major obstacle to the application of such equations to general dispersion problems. The present problem indicates that, independent of the Eulerian distribution of velocities at a point, many different models exist with a distinguishing characteristic being the time-averaged mean angular momentum of a Lagrangian particle described by each model. We can no longer hope to simply constrain even one-particle stochastic equations in complex non-isotropic conditions just in terms of one-point Eulerian velocity statistics, but other parameters like angular momentum, which is essentially Lagrangian in nature and is known to be a measure of skew diffusion (Moffatt 1983), must be taken into account.

For simplicity we use Gaussian statistics for the Eulerian distribution of velocities at a point (homogeneity means that this distribution is the same for any point in space). We also restrict our attention to linear models (whenever a choice is possible). This allows for solutions in terms of simple functions and displays the full complexity anticipated from nonlinear solutions in any case.

2. Stochastic model equations

Following Thomson (1987), let $\mathrm{d}t$ be an infinitesimal time increment. For such time increments the stochastic equations describing the evolution of the path of a fluid particle are

$$\left.\begin{aligned} \mathrm{d}u_i &= a_i\,\mathrm{d}t + \alpha\,\mathrm{d}W_i, \\ \mathrm{d}x_i &= u_i\,\mathrm{d}t, \end{aligned}\right\} \tag{1}$$

where $\boldsymbol{x}$ is position, $\boldsymbol{u}$ is velocity, $\boldsymbol{a}$ is the acceleration-drift vector of a fluid particle, $\mathrm{d}\boldsymbol{W}$ is white noise and α is a parameter. The drift vector, $\boldsymbol{a}$, in the equation for rate-of-change of velocity, is a function of the velocity itself and other parameters. The value of α and the appropriate scale for the Eulerian velocity fluctuation, σ_u, define an integral time scale for this framework. In Thomson's formulation we are supposing that the time scale for viscous effects, t_η say, is much smaller than any time increment we consider. Thus the smallest-scale effects considered (dominated by the white noise in (1)) are inertial-range scales which have precise properties based on the rate of energy dissipation, $\bar{\epsilon}$ and, moreover, are isotropic.

Kolmogorov scaling (Inoue 1952) implies that

$$\langle \mathrm{d}u_i\,\mathrm{d}u_j \rangle = C_0\,\bar{\epsilon}\delta_{ij}\,\mathrm{d}t + o(\mathrm{d}t),$$

for some universal constant C_0, which has a value of approximately 6 or 7 (Sawford 1991; Pope 1994) although other estimates range as low as 2 (Anand & Pope 1985). From the leading order of the mean square of equation (1), we therefore have $\alpha^2 = C_0\,\bar{\epsilon}$. These results are true even when intermittency is explicitly considered, but higher-order even moments of $\mathrm{d}u_i$ are then proportional to non-integer powers of $\mathrm{d}t$.

Note that there is no broken reflectional symmetry at this order. What is implied here is that the smallest meaningful scale of motion in the turbulence, which is the result of the ubiquitous turbulent cascade, is dominated by local isotropic interactions and only 'feels' broken reflectional symmetry at higher orders.

In this paper we explicitly break reflectional symmetry, while maintaining the simplest possible flow consistent with this, namely non-reflectional axisymmetric flow. These characteristics are imposed via the drift term, $\boldsymbol{a}$, in (1). A higher degree of

https://doi.org/10.1017/S002211209600393X Published online by Cambridge University Press

symmetry is spherical symmetry lacking reflectional symmetry (Batchelor 1953), but it is not possible to treat this problem with the simple model (1) employed here, which will be evident later. In addition, axisymmetry is the least level of complexity at which the important effect of skew diffusion occurs (Moffatt 1983).

3. Fokker–Planck equations and drift terms

Model (1) is equivalent (Gardiner 1983) to the equation for the transition density for velocity and position, P, which satisfies the Fokker–Planck equation

$$\frac{\partial P}{\partial t}+\frac{\partial u_i P}{\partial x_i}+\frac{\partial a_i P}{\partial u_i}=\tfrac{1}{2}\alpha^2\frac{\partial^2 P}{\partial u_j\,\partial u_j}. \tag{2}$$

The stationary equilibrium solution satisfies

$$\frac{\partial a_i P_E}{\partial u_i}=\tfrac{1}{2}\alpha^2\frac{\partial^2 P_E}{\partial u_j\,\partial u_j}. \tag{3}$$

Using the Gaussian distribution

$$P_E=(2\pi\sigma_u^2)^{-3/2}\exp\left(-\frac{u_i u_i}{2\sigma_u^2}\right), \tag{4}$$

we find that

$$a_i=-\frac{1}{2}\frac{\alpha^2}{\sigma_u^2}u_i.$$

However components may be added to this drift vector, say $\tilde{a}$, provided that

$$\frac{\partial \tilde{a}_i P_E}{\partial u_i}=0.$$

The drift term is only unique in isotropic turbulence when $\tilde{a}$ must vanish (Borgas & Sawford 1994*b*). However, suppose that the flow is axisymmetric and that there is some 'handedness' or chirality about some axis indicated by the direction $\boldsymbol{\Omega}$.† The well-mixed condition (Thomson 1987) allows

$$a_i=-\frac{1}{2}\frac{\alpha^2}{\sigma_u^2}u_i+\epsilon_{ijk}\Omega_j u_k \tag{5}$$

as a general linear solution. Nonlinear solutions are also (trivially) available, but we shall not consider these. The non-uniqueness is reflected by the fact that the length of $\boldsymbol{\Omega}$ is arbitrary; its magnitude $|\boldsymbol{\Omega}|$ is a parameter determining the flow. The well-mixed condition ensures that initially uniform mixtures of tracer material are not unmixed by the (modelled) fluid motions. This is essential for a good dispersion model.

We are supposing here that the change from full isotropy is minimal, i.e. we maintain symmetry with respect to rotations of coordinate axes about $\boldsymbol{\Omega}$ but do not have

† The flow is symmetric when reflected in planes containing $\boldsymbol{\Omega}$. However, reflections in the plane to which $\boldsymbol{\Omega}$ is normal, are not symmetric (i.e. when we hold a mirror orthogonal to $\boldsymbol{\Omega}$ we observe a change in flow screw-sense properties).

https://doi.org/10.1017/S002211209600393X Published online by Cambridge University Press

reflectional symmetry. However, the Eulerian velocity statistics chosen in (4) are appropriate for fully isotropic turbulence, i.e.

$$\langle u_i u_j \rangle = \sigma_u^2 \delta_{ij};$$

this choice is made in order to highlight particularly the impact of broken reflectional symmetry. Studies of rotating homogeneous turbulence (Zeman 1994) suggest that this form is appropriate and that other, often two-point, quantities are more substantially altered by rotational effects. However, the analysis even for axisymmetric Eulerian distributions,

$$\langle u_i u_j \rangle = (\vartheta_1 - \vartheta_2)\frac{\Omega_i \Omega_j}{\Omega^2} + \vartheta_2 \delta_{ij},$$

where ϑ_1, ϑ_2 are some constants (with dimensions of σ_u^2), produces essentially the same results when reflectional symmetry is broken. It is possible to adjust all the algebra for general axisymmetry with essentially no new features emerging as part of the linear solution. In reflectionally symmetric turbulence with axisymmetry there is a unique linear model, but non-uniqueness arises if nonlinear models are considered.

Note that in the context of rotating turbulence, the reflection-breaking term in (5) has the appearance of a Coriolis acceleration induced in a frame rotating about $\boldsymbol{\Omega}$ with angular frequency $\frac{1}{2}\Omega$. The identification with Coriolis acceleration (again stressing that $\boldsymbol{a}$ is a stochastic inertial-range drift term and not strictly an acceleration) is at best only partly true because if we formulate the dispersion problem relative to an observer in a non-rotating frame then we might expect the terms in $\boldsymbol{a}$ involving $\boldsymbol{\Omega}$ to be absent. However, in this frame the observer sees a non-trivial mean flow and in consequence can never associate the flow with a homogeneous isotropic one, thereby allowing a unique specification of the stochastic equation through the well-mixed equation. Thus although the rotating turbulence example is perhaps the most easily realized non-reflectional case approximated by the present model problem, the magnitude of $\boldsymbol{\Omega}$ in the stochastic equation is not simply related to the rotation rate of the turbulence. The implicit relationship which must exist, if only approximately, is beyond the scope of this paper although the issue is briefly reconsidered below (§6).

The imposed direction $\boldsymbol{\Omega}$ is essential for introducing terms in (5) that lack reflectional symmetry. It is impossible to construct such terms otherwise: the only vector direction available for prescribing $\boldsymbol{a}$ (and $\tilde{\boldsymbol{a}}$) would then be $\boldsymbol{u}$ itself. Thus, as we foreshadowed, the non-reflectional spherically symmetric case cannot be treated by the present analysis.

Note that in the case of Gaussian one-particle statistics, the stress tensor, $\langle u_i u_j \rangle$, contains no information about reflectional symmetry because it is by definition symmetric. To invoke reflectional symmetry breaking via P_E, skewed non-Gaussian distributions must be used, but then we necessarily develop nonlinear Lagrangian models which require numerical solution. Even then non-trivial skewness is only possible with some distinguished direction like $\boldsymbol{\Omega}$, so there is no escaping the need for axisymmetry by this route. A wide range of qualitative behaviour is evidently possible with linear models by breaking the symmetry of the drift term $\boldsymbol{a}$ as above, and unless other evidence (empirical, numerical or from more sophisticated theory) suggests broader forms of behaviour are needed, linear models are the most worthy of detailed study.

https://doi.org/10.1017/S002211209600393X Published online by Cambridge University Press

4. Solving the linear equation

The general linear stochastic equation can be represented in non-dimensional form by

$$\mathrm{d}u_i = -A_{ij}u_j\,\mathrm{d}t + \sqrt{2}\,\mathrm{d}W_i,$$

where velocities are normalized with σ_u and time with $t_L = 2\sigma_u^2/C_0\bar{\epsilon}$. The matrix A_{ij} has the form

$$A_{ij} = \begin{pmatrix} 1 & 0 & 0 \\ 0 & 1 & \omega \\ 0 & -\omega & 1 \end{pmatrix},$$

where $\omega = |\Omega|\,t_L$ is an arbitrary dimensionless constant. We have here, without loss of generality, chosen the $\boldsymbol{\Omega}$-direction to coincide with the x_1 (or u_1)-direction.

The dynamics of the process is that a change of velocity $\boldsymbol{u}$ at each instant is made up of an isotropic random 'acceleration', and an accompanying 'drag' proportional to velocity and a right-handed rotation about $\boldsymbol{\Omega}$. Despite the isotropy of the dominant accelerations, and of Eulerian velocity statistics, the drift term (drag and rotation) persists for integral time scales and thus exert a significant influence on the processes, giving rise for example to net angular momentum for the particle.

The linear equation may be solved with a transformation: let

$$u_i = Q_{ij}v_j,$$

where the columns of Q_{ij} are the eigenvectors of A_{ij}. The eigenvalues of A_{ij}, given by

$$|A_{ij} - \lambda\delta_{ij}| = (1-\lambda)\,((1-\lambda)^2 + \omega^2) = 0,$$

are $\lambda = 1, 1+\mathrm{i}\omega$ and $1-\mathrm{i}\omega$, i.e. one real and one complex-conjugate pair. Obviously the complex-conjugate pair leads to oscillations in the solution (with frequency ω). The matrix Q_{ij} thus has the form

$$Q_{ij} = \frac{1}{\sqrt{2}}\begin{pmatrix} \sqrt{2} & 0 & 0 \\ 0 & 1 & 1 \\ 0 & -\mathrm{i} & \mathrm{i} \end{pmatrix},$$

which has the inverse

$$Q_{ij}^{-1} = \frac{1}{\sqrt{2}}\begin{pmatrix} \sqrt{2} & 0 & 0 \\ 0 & 1 & \mathrm{i} \\ 0 & 1 & -\mathrm{i} \end{pmatrix}.$$

The equation for v has the form

$$\mathrm{d}v_i = -B_{ij}v_j\,\mathrm{d}t + \sqrt{2}\,Q_{ij}^{-1}\,\mathrm{d}W_j,$$

where $B_{ij} = Q_{ik}^{-1}A_{kl}Q_{lj}$ is the diagonal matrix

$$B_{ij} = \begin{pmatrix} 1 & 0 & 0 \\ 0 & 1-\mathrm{i}\omega & 0 \\ 0 & 0 & 1+\mathrm{i}\omega \end{pmatrix}.$$

Thus the system is

$$\left.\begin{aligned} \mathrm{d}v_1 &= -v_1\,\mathrm{d}t + \sqrt{2}\,\mathrm{d}W_1, \\ \mathrm{d}v_2 &= -(1-\mathrm{i}\omega)\,v_2\,\mathrm{d}t + (\mathrm{d}W_2 + \mathrm{i}\,\mathrm{d}W_3), \\ \mathrm{d}v_3 &= -(1+\mathrm{i}\omega)\,v_3\,\mathrm{d}t + (\mathrm{d}W_2 - \mathrm{i}\,\mathrm{d}W_3). \end{aligned}\right\} \tag{6}$$

https://doi.org/10.1017/S002211209600393X Published online by Cambridge University Press

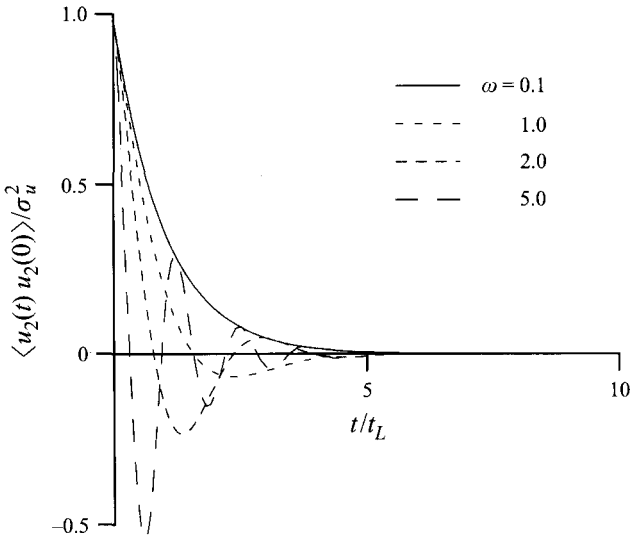


FIGURE 1. Velocity autocorrelation of the transverse velocity components (in the plane orthogonal to $\boldsymbol{\Omega}$) for the linear model calculated for a sequence of ω-values, where $\omega = |\boldsymbol{\Omega}|\,t_L$. The longitudinal velocity autocorrelation parallel to $\boldsymbol{\Omega}$, given by $\omega = 0$, is approximately equivalent to $\omega = 0.1$.

Note that v_2 and v_3 are a complex-conjugate pair, thus it is sufficient to solve for v_1 and v_2. The solution for v_1 is obvious and we simply obtain

$$\langle v_1(t)\,v_1(0)\rangle = \langle v_1^2(0)\rangle\,\mathrm{e}^{-t}.$$

Similarly we integrate to find

$$v_2(t) = \mathrm{e}^{-(1-\mathrm{i}\omega)\,t}\,v_2(0) + \int_0^t \mathrm{e}^{-(1-\mathrm{i}\omega)\,(t-t')}\,(\mathrm{d}W_2' + \mathrm{i}\,\mathrm{d}W_3'),$$

so that

$$\langle v_2(t)\,v_2(0)\rangle = \langle v_2^2(0)\rangle\,\mathrm{e}^{-(1-\mathrm{i}\omega)\,t}$$

and

$$\langle v_2(t)\,\overline{v_2(0)}\rangle = \langle v_2(0)\,\overline{v_2(0)}\rangle\,\mathrm{e}^{-(1-\mathrm{i}\omega)\,t}.$$

Immediately we have

$$\langle v_3(t)\,v_3(0)\rangle = \overline{\langle v_2^2(0)\rangle}\,\mathrm{e}^{-(1+\mathrm{i}\omega)\,t},$$

where the overline indicates complex conjugation.

We wish to construct the velocity autocorrelation in terms of real velocities; thus

$$\langle u_i(t)\,u_j(0)\rangle = Q_{ik}\,Q_{jl}\,\langle v_k(t)\,v_l(0)\rangle,$$

but since

$$\langle u_i(0)\,u_j(0)\rangle = \delta_{ij},$$

which leads to the results

$$\langle v_1^2(0)\rangle = 1, \quad \langle v_2^2(0)\rangle = 0, \quad \langle v_2(0)\,\overline{v_2(0)}\rangle = 1,$$

we finally have

$$\langle u_i(t)\,u_j(0)\rangle = \mathrm{e}^{-t}\begin{pmatrix} 1 & 0 & 0 \\ 0 & \cos\omega t & -\sin\omega t \\ 0 & \sin\omega t & \cos\omega t \end{pmatrix}. \tag{7}$$

The oscillatory diagonal components of the velocity autocorrelation are shown in figure 1. The off-diagonal elements are shown in figure 2.

https://doi.org/10.1017/S002211209600393X Published online by Cambridge University Press

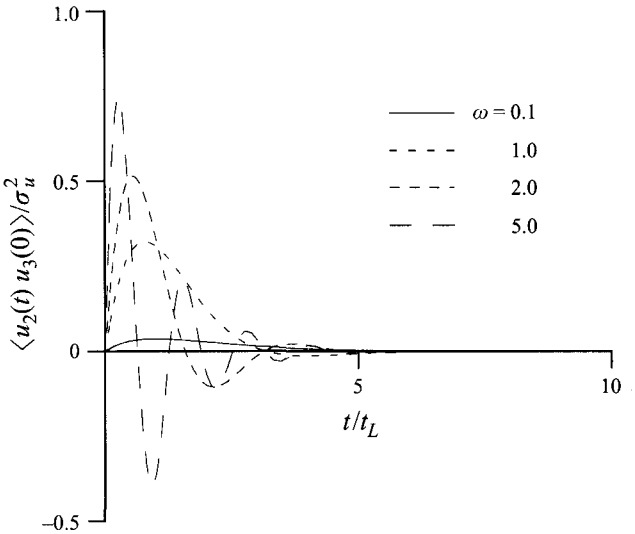


FIGURE 2. Correlation of the off-diagonal transverse velocity components (in the plane orthogonal to $\boldsymbol{\Omega}$) for the linear model calculated for a sequence of ω-values.

The corresponding dispersion is also anisotropic and is determined from the velocity autocorrelation. Let

$$\langle u_i(t_1)\, u_j(t_2)\rangle = R_{ij}(t_1 - t_2) \quad \text{for} \quad t_1 \geqslant t_2.$$

Consequently, when $t_1 < t_2$

$$\langle u_i(t_1)\, u_j(t_2)\rangle = R_{ji}(t_2 - t_1).$$

The dispersion from the origin follows from

$$\langle x_i(t)\, x_j(t)\rangle = \int_0^t \int_0^t \langle u_i(t_1)\, u_j(t_2)\rangle \, \mathrm{d}t_1 \, \mathrm{d}t_2,$$

$$= \int_0^t \int_0^{t_1} R_{ij}(t_1 - t_2)\, \mathrm{d}t_1 \, \mathrm{d}t_2 + \int_0^t \int_{t_1}^t R_{ji}(t_2 - t_1)\, \mathrm{d}t_1 \, \mathrm{d}t_2,$$

whereupon

$$\langle x_i(t)\, x_j(t)\rangle = \int_0^t (t-\tau)\,(R_{ij}(\tau) + R_{ji}(\tau))\, \mathrm{d}\tau.$$

Thus

$$\langle x_i(t)\, x_j(t)\rangle = 2 \begin{pmatrix} \int_0^t (t-\tau)\, \mathrm{e}^{-\tau} \mathrm{d}\tau & 0 & 0 \\ 0 & \int_0^t (t-\tau) \cos\omega\tau\, \mathrm{e}^{-\tau}\, \mathrm{d}\tau & 0 \\ 0 & 0 & \int_0^t (t-\tau) \cos\omega\tau\, \mathrm{e}^{-\tau}\, \mathrm{d}\tau \end{pmatrix},$$

i.e.

$$\left.\begin{aligned} \langle x_1^2\rangle &= 2(t + \mathrm{e}^{-t} - 1), \\ \langle x_2^2\rangle &= \frac{2}{1+\omega^2}\left(t - \frac{2\omega}{1+\omega^2}\mathrm{e}^{-t}\sin\omega t + \frac{\omega^2-1}{1+\omega^2}(1 - \mathrm{e}^{-t}\cos\omega t)\right), \\ \langle x_3^2\rangle &= \frac{2}{1+\omega^2}\left(t - \frac{2\omega}{1+\omega^2}\mathrm{e}^{-t}\sin\omega t + \frac{\omega^2-1}{1+\omega^2}(1 - \mathrm{e}^{-t}\cos\omega t)\right). \end{aligned}\right\} \tag{8}$$

https://doi.org/10.1017/S002211209600393X Published online by Cambridge University Press

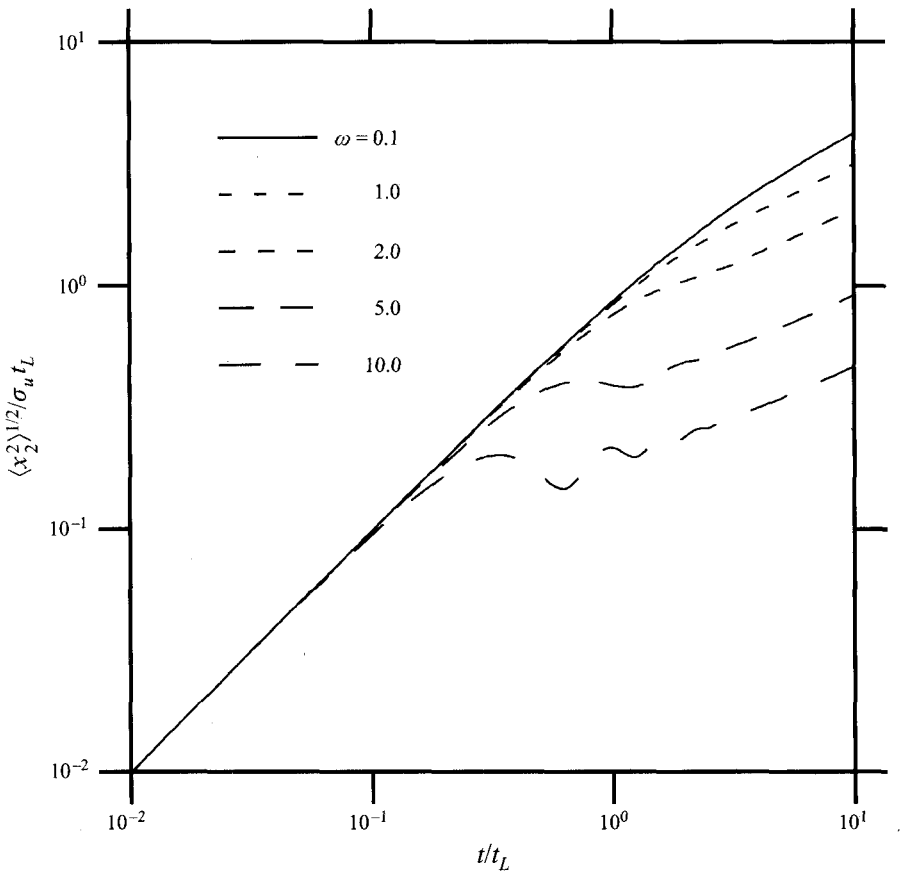


FIGURE 3. As for figure 1, but showing the dispersion in the plane orthogonal to $\boldsymbol{\Omega}$. The along-$\boldsymbol{\Omega}$ dispersion, given by $\omega = 0$, is approximately equivalent to $\omega = 0.1$.

The dispersion in the x_1-direction, parallel to the 'handedness', is unaltered by the anisotropy. The dispersion in the plane orthogonal to the 'handedness' (i.e. the x_2, x_3-plane) is described by the function

$$D_{\Omega}(t) = \frac{2}{1+\omega^2}\left(t - \frac{2\omega}{1+\omega^2}\mathrm{e}^{-t}\sin\omega t + \frac{\omega^2-1}{1+\omega^2}(1-\mathrm{e}^{-t}\cos\omega t)\right),$$

which is shown in figure 3 to be very much smaller than the dispersion in the x_1-direction. Note that in the limit $\omega \to 0$ we recover the normal isotropic results. Also in the small-time limit, $D_{\Omega} = t^2 + O(t^3)$ has the leading-order independent of the anisotropy. On the other hand, in the limit $\omega \to \infty$, the dispersion is amazingly suppressed in the anisotropic directions; in fact

$$D_{\Omega}(t) = \frac{2}{\omega^2}\left(t + 1 - \mathrm{e}^{-t}\cos\omega t - \frac{2}{\omega}\mathrm{e}^{-t}\sin\omega t\right) + O(\omega^{-4}).$$

Thus the linear growth is forestalled until $t \gg 1$, with oscillations appearing for times such that $\omega^{-1} \ll t \ll 1$ provided that ω is not too small, and with the slope of the eventual linear mean-square growth inversely proportional to the square of frequency.

Because of the different dispersion in different orthogonal directions we find that an initially spherical (on average) blob of material becomes drawn out into a 'needle'-shaped mean distribution, i.e. larger dispersion in one direction (along the axis of

https://doi.org/10.1017/S002211209600393X Published online by Cambridge University Press

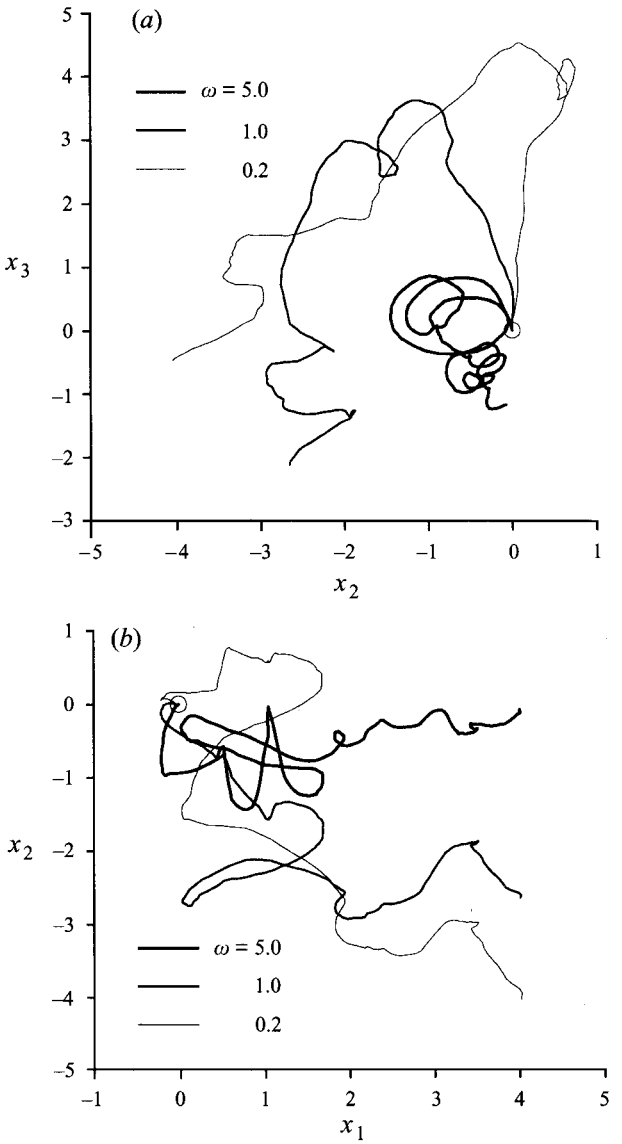


FIGURE 4. A selection of trajectories for different magnitudes of $\boldsymbol{\Omega}$. Projections of the trajectories beginning at the origin (marked as a circle) are shown in two orthogonal planes; a clear spiralling tendency is evident in the plane orthogonal to $\boldsymbol{\Omega}$, (*a*), but not in the plane containing $\boldsymbol{\Omega}$, (*b*). The three curves in each plane correspond to the same sequence of white noise in (1) and the differences are solely due to the reflection-breaking term in the drift term with different ω-values.

anisotropy) with cylindrically symmetric dispersion in planes orthogonal to this direction.

Figure 4 shows some trajectories of particles in these flows: (*a*) shows a projection in the plane normal to $\boldsymbol{\Omega}$, and (*b*) in a plane containing $\boldsymbol{\Omega}$. The figure shows the influence of increasing ω. Each trajectory corresponds to the same sequence of white noise in (1), but the spiralling effects differ because of changes of ω in (5). Clearly, for

https://doi.org/10.1017/S002211209600393X Published online by Cambridge University Press

large ω, the trajectories spiral around the direction $\boldsymbol{\Omega}$ with a clear (right) handedness (note that if the particle's trajectory moves along the positive $\boldsymbol{\Omega}$-direction then the trajectory itself resembles a right-handed screw but if the trajectory moves along the negative $\boldsymbol{\Omega}$-direction it is a left-handed screw). This is responsible for both the oscillations of autocorrelations and the dramatic reduction of dispersion in the plane orthogonal to $\boldsymbol{\Omega}$.

The evident consequence of broken reflectional symmetry (and therefore possibly of helicity) is the reduction of dispersive power. Particle paths meander according to the random impetus of the smallest eddies, but are drawn around into spirals by the screw sense of the flow. Thus the particles remain close to the axis (through the origin in the $\boldsymbol{\Omega}$-direction) for much longer than if the excursions of the particle rotate as much to the left around the axis as to the right. The dispersive power in spherically symmetric flows with helicity, which is outside the scope of our model, and is what Kraichnan (1977) considers, is apparently affected in the opposite sense to the axisymmetric case. This seems hard to understand. If for example the helical nature of spherically symmetric flow were to consist of a field of local flows like randomly orientated right-handed screws, there is apparently at least a small-scale analogue of the effect described by our axisymmetric model which should therefore diminish dispersion. Moreover, Kraichnan's model and subsequent developments of it (Drummond, Duane & Horgan 1984) effectively correspond to much smaller Reynolds number than we envisage as appropriate for our model and therefore the comparison is not necessarily meaningful.

5. Fluxes in a uniform gradient of passive tracer

Yet again we follow the spirit of Taylor (1921) and consider the evolution of passive tracer (say θ) advected by our turbulent flow, where θ is initially present as an unbounded uniform gradient, i.e. the concentration at time $t = 0$ is $Sx_i z_i$, where $\boldsymbol{z}$ is a unit vector in the direction of the gradient. This ideal tracer distribution has also been considered by Corrsin (1951) and in wind-tunnel flows such distributions can be created approximately: the so-called *toaster* configuration (Jayesh & Warhaft 1992) consisting of a vertical series of parallel heated ribbon sources arranged in a plane normal to the oncoming flow and where each ribbon is heated at a rate slightly greater than the one below it. The present study additionally has broken reflectional symmetry of the flow which has not been studied experimentally for a uniform passive-tracer gradient. When such a distribution is acted upon by homogeneous turbulence (for example, by introducing a uniform grid downstream of the 'toaster' source), the subsequent mean concentration field at time t is

$$\langle\theta(\boldsymbol{x})\rangle = Sz_i \int x_{0i}\, P(\boldsymbol{x}, t; \boldsymbol{x}_0)\, \mathrm{d}^3 \boldsymbol{x}_0 = Sx_i z_i - Sz_i \int (x_i - x_{0i})\, P(\boldsymbol{x}, t; \boldsymbol{x}_0)\, \mathrm{d}^3 \boldsymbol{x}_0 = Sx_i z_i,$$

which is evidently unchanged from the initial distribution. The generalized transition probability density, P, is simply Gaussian with vanishing mean displacements and the mean-square displacements as given in (8).

Despite the simplicity of an unchanging mean concentration, the underlying physics are that this situation is maintained by non-trivial fluxes of material: the fluxes are

$$\langle u_i \theta\rangle = Sz_j \int u_i x_{0j}\, P(\boldsymbol{u}, \boldsymbol{x}, t; \boldsymbol{x}_0)\, \mathrm{d}^3 \boldsymbol{x}_0\, \mathrm{d}^3 \boldsymbol{u},$$

https://doi.org/10.1017/S0022112096003931X Published online by Cambridge University Press

which may be expressed (using homogeneity) as

$$\langle u_i \theta \rangle = -Sz_j \int_0^t R_{ij}(\tau)\,\mathrm{d}\tau = -F_{ij} Sz_j, \tag{9}$$

where

$$F_{ij} = \begin{pmatrix} 1-\mathrm{e}^{-t} & 0 & 0 \\ 0 & \dfrac{1-\mathrm{e}^{-t}\cos\omega t+\omega\,\mathrm{e}^{-t}\sin\omega t}{1+\omega^2} & -\dfrac{\omega-\omega\,\mathrm{e}^{-t}\cos\omega t-\mathrm{e}^{-t}\sin\omega t}{1+\omega^2} \\ 0 & \dfrac{\omega-\omega\,\mathrm{e}^{-t}\cos\omega t-\mathrm{e}^{-t}\sin\omega t}{1+\omega^2} & \dfrac{1-\mathrm{e}^{-t}\cos\omega t+\omega\,\mathrm{e}^{-t}\sin\omega t}{1+\omega^2} \end{pmatrix}.$$

In general, for any direction z of the scalar gradient there is a flux down the gradient and a flux perpendicular to the gradient (in the direction $\boldsymbol{\Omega} \times z$). However, if z is aligned with $\boldsymbol{\Omega}$ we get no transverse fluxes (perpendicular to z), and there is only the usual flux down the gradient.

The initial development (to $O(t^2)$) of the fluxes follows as

$$F_{ij} = \begin{pmatrix} t-\frac{1}{2}t^2 & 0 & 0 \\ 0 & t-\frac{1}{2}t^2 & -\frac{1}{2}\omega t^2 \\ 0 & \frac{1}{2}\omega t^2 & t-\frac{1}{2}t^2 \end{pmatrix},$$

which is approximately diagonal for small times, and the steady state (for large times) is

$$F_{ij} = \begin{pmatrix} 1 & 0 & 0 \\ 0 & \dfrac{1}{1+\omega^2} & -\dfrac{\omega}{1+\omega^2} \\ 0 & \dfrac{\omega}{1+\omega^2} & \dfrac{1}{1+\omega^2} \end{pmatrix}.$$

In general, the off-diagonal fluxes vanish when $\omega = 0$. However, for any finite ω there will be off-diagonal elements; these have maximal intensity when $\omega = 1$ and decrease as ω increases. In addition, the diagonal elements corresponding to the directions orthogonal to the $\boldsymbol{\Omega}$-direction have maximal intensity for zero ω and decrease monotonically with increasing ω, i.e. the fluxes orthogonal to $\boldsymbol{\Omega}$ can be made very small.

It is straightforward to understand the physical origin of the off-diagonal fluxes. The flux at any point is determined by the average over all trajectories passing through that point. The off-diagonal flux is illustrated schematically in figure 5 and is explained by considering two 'average' trajectories, one commencing above the measurement point M and one (by symmetry) commencing below it. The two trajectories represent independent realizations and are not concurrent. Because of the biased symmetry of the flow, with respect to $\boldsymbol{\Omega}$ 'out of the page', the right-handed sense of rotation of both trajectories dominates, but note that at the point M there is no net Eulerian velocity. The average transport at M for a mean gradient in the z-direction occurs because, in each case, concentration is conserved along the trajectory, but is greater for the upper trajectory. Thus on average, trajectories commencing above the measurement point transport hotter fluid to the right and trajectories below the measurement point transport colder fluid to the left. The net effect is a flux of warmer fluid to the right, i.e. a positive cross-gradient flux. Of course, there is always the simultaneous down-gradient flux.

https://doi.org/10.1017/S002211209600393X Published online by Cambridge University Press

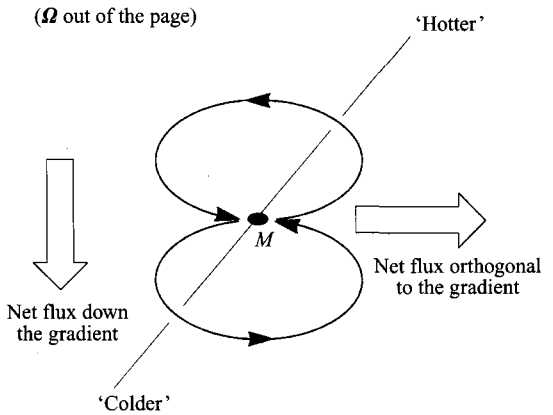


FIGURE 5. Schematic of transport with a preferred spiralling tendency. The flux at measurement point M is considered. Two typical trajectories are shown passing through M for independent realizations. The dominant right-handed motions (with $\boldsymbol{\Omega}$ coming out of the page) give these trajectories their sense of circulation. The upper trajectory transports 'hotter' fluid to the right at M, the lower trajectory transports 'colder' fluid to the left, resulting in a net positive flux to the right at M, i.e. a flux orthogonal to the gradient.

Moffatt (1983) highlighted skew-diffusion as an important transport characteristic. It can only occur in axisymmetric turbulence (i.e. with some $\boldsymbol{\Omega}$-direction), otherwise the F_{ij} tensor defined in (9) cannot have off-diagonal elements. Thus skew-diffusion is not a phenomenon associated with non-reflectional spherically symmetric turbulence. Of course, skew diffusion is possible in flows without any significant symmetry, but the overall complexity of such flows would obscure these transport effects.

6. Angular momentum

The effects that we have described depend critically on the parameter $\boldsymbol{\Omega}$ but we have not ascribed a simple dynamical or kinematical property to this vector. In §3 $\boldsymbol{\Omega}$ is considered as an implicit property of the homogeneous non-reflectional flow which could not be easily related to the one-point Eulerian velocity statistics, nor, for example, to the bulk rotation rate of homogeneous turbulence (Zeman 1994) in that physical manifestation of broken reflection.

The most appropriate interpretation of $\boldsymbol{\Omega}$ (from Moffatt 1983) is that it is proportional to the mean angular momentum of a Lagrangian particle (the Eulerian field has no net angular momentum). Let $\boldsymbol{X}$ be the Lagrangian position of a particle which is at the origin at time $t = 0$ and let $\boldsymbol{V}$ be the corresponding Lagrangian velocity. The mean angular momentum is

$$h_i(t) = \epsilon_{ijk} \langle X_j V_k \rangle = \epsilon_{ijk} \int_0^t R_{kj}(t') \, \mathrm{d}t',$$

which is dimensionless according to the scale given above. Note the ordering of the indices. The solution obtained above for the velocity autocorrelation, $R_{ij}(\tau)$, is given in (7), and when integrated as in (9) gives the long-time angular momentum

$$h_i(\infty) = \frac{2}{1+\omega^2} \omega_i \quad (\boldsymbol{\omega} = t_L \boldsymbol{\Omega}),$$

https://doi.org/10.1017/S002211209600393X Published online by Cambridge University Press

which relates $\boldsymbol{\Omega}$ in (5) to a physical property. The long-time-average angular momentum,

$$\bar{h}_i = \lim_{T\to\infty} \frac{1}{T}\int_0^T h_i(t)\,\mathrm{d}t,$$

will clearly approach $h_i(\infty)$ after the initial transients have died away (on the time scale t_L). Note that according to these results (from a linear model), the magnitude of $\bar{\boldsymbol{h}}$ is bounded by unity (for $|\omega| = 1$). Consequently, if a real physical flow were to correspond to mean (dimensionless) angular-momentum magnitude greater than unity, then at the very least a nonlinear version of model (1) must be used to describe the behaviour. For a nonlinear model

$$h_i(\infty) = H(\omega)\,\omega_i,$$

where $H(\omega)$ is an unknown functional of the nonlinear form of $\boldsymbol{a}$ in (1). Thus there is still a direct connection between the direction of the angular momentum and the arbitrary direction $\boldsymbol{\Omega}$; however, the precise constant of proportionality is subject to model (or equivalently flow) details.

Thus we have posed a flow where an important physical property is the mean angular momentum of fluid particles, $\bar{\boldsymbol{h}}$, rather than the pseudo-scalar helicity (see § 1), which more naturally reflects properties of two-point characteristics of turbulence. However, it is impossible to measure the characteristic angular momentum with one-point velocity measurements (nor is it possible to deduce two-point statistics from such measurements). The implication is that one-particle Lagrangian measurements must be made in order to close the Lagrangian model, i.e. to specify it completely. Thus to prescribe a Lagrangian model we must know the Lagrangian statistics: that is, in general the Lagrangian stochastic model cannot be specified uniquely in terms of one-point Eulerian velocity statistics.

7. Conclusions

We have presented a simple model of turbulent dispersion in non-reflectional axisymmetric flows, which is relevant in a number of (ideal) practical contexts. The dispersion has a number of interesting features:

the Lagrangian velocity autocorrelation oscillates as it magnitude abates;
the dispersion also oscillates, but more weakly;
the dispersion is significantly reduced with broken reflection;
particle trajectories have a pronounced spiral structure with broken reflection (which is why the dispersion quantities oscillate);
skew diffusion arises inevitably as a consequence of broken reflection in axisymmetric turbulence;
the mean angular momentum of fluid particles is an important parameter.

These conclusions are all made with a remarkably simple model which gives exact solutions; the model results from rational idealizations of flows which are nearly statistically homogeneous and axisymmetric, but lack reflectional symmetry. Such idealizations are not overly gross approximations of a number of real flows.

What is complex, however, is the interpretation of reflectional symmetry in terms of the often-used Eulerian diagnostic of turbulence–helicity. Flows with helicity necessarily lack reflectional symmetry (but the converse is not so clear). However, the one-particle Lagrangian model which is considered here cannot be easily related to helicity, which is more naturally a two-particle property. Rather our fundamental physical parameter is the mean angular momentum of fluid particles, which gives rise to all the properties described above when it is non-zero.

https://doi.org/10.1017/S002211209600393X Published online by Cambridge University Press

The angular momentum in our linear model is bounded. Near its maximal value ($|\omega| = 1$) there is a balance between the spiralling rate around the axis ($\boldsymbol{\Omega}$) and the excursion from the axis. For smaller $|\omega|$, the particles spiral too slowly to have significant angular momentum, and for large $|\omega|$, particle trajectories spiral tightly around the axis parallel to $\boldsymbol{\Omega}$ drawn through an 'initial' starting point, i.e. there are much reduced excursions orthogonal to $\boldsymbol{\Omega}$ and consequently small angular momentum. The dispersion orthogonal to $\boldsymbol{\Omega}$ is enormously reduced because of these spirals.

Flows with larger mean angular momentum than the maximal magnitude cannot be described by linear models and necessarily involve nonlinear effects. It is unlikely that the simple linear models considered here could predict an absolute bound on angular momentum. It would be interesting to assess whether or not larger angular momentum could result from nonlinear stochastic models (i.e. by making components of $\boldsymbol{\Omega}$ scalar functions of $\boldsymbol{u}$).

It is clear that these results have important ramifications. Estimates of dispersion cannot be qualitatively constructed just on the basis of velocity fluctuations and Lagrangian time scales, but, in addition, the mean rotational sense of the turbulent eddies, if of some preferred sense, can drastically diminish dispersion. Thus eddy diffusivities, which are commonly used approximations in complex flows, depend critically upon the local angular momentum $\boldsymbol{h}$ (i.e. helicity effects) as well as σ_u and the time scale. If some prognostic estimate of $\boldsymbol{h}$ can be made, much improved parameterizations of turbulent dispersion are perhaps possible.

Furthermore, complex stochastic models of non-isotropic turbulence are hampered by a non-uniqueness problem. Many recent avenues of research have treated this as just the lack of a further constraint based on P_E in order to select the model (Borgas & Sawford 1994*b*; Flesch & Wilson 1992). The philosophy has been that, when given $P_E(\boldsymbol{u})$, a unique model will result provided we have enough constraints based on it and the dispersion that ensues from it. However, the present situation has a given Gaussian P_E but the non-uniqueness is related to physical properties unconnected with P_E. For example, if we have the additional information that the mean angular momentum of fluid particles is zero, then we again have a unique model. Thus it is clear that further information than is given by P_E alone is necessary for the full characterization of a Lagrangian dispersion model.

Of course, a real fluid flow governed by the Navier–Stokes equations is likely to have some explicit relation between P_E, the mean angular momentum $\boldsymbol{h}$ (hence $\boldsymbol{\Omega}$), and the imposed forcing. The derivation of this relation would be an extremely worthwhile problem in statistical fluid mechanics.

REFERENCES

ANAND, M. S. & POPE, S. B. 1985 Diffusion behind a line source in grid turbulence. In *Turbulent Shear Flows* (ed. L. J. S. Bradbury, F. Durst, B. E. Launder, F. W. Schmidt & J. H. Whitelaw), vol. 4. Springer.

ANGELL, J. K., PACK, D. H. & DICKSON, C. R. 1967 A Lagrangian study of helical circulations in the planetary boundary layer. *J. Atmos. Sci.* **25**, 707–717.

BATCHELOR, G. K. 1953 *The Theory of Homogeneous Turbulence*. Cambridge University Press.

BORGAS, M. S. & SAWFORD, B. L. 1991 The small-scale structure of acceleration correlations and its role in the statistical theory of turbulent dispersion. *J. Fluid Mech.* **228**, 295–320.

BORGAS, M. S. & SAWFORD, B. L. 1994*a* Stochastic equations with multifractal increments for modelling turbulent dispersion. *Phys. Fluids* A **6**, 618–633.

BORGAS, M. S. & SAWFORD, B. L. 1994*b* A family of models for two-particle dispersion in isotropic homogeneous stationary turbulence. *J. Fluid Mech.* **279**, 69–99.

https://doi.org/10.1017/S002211209600393X Published online by Cambridge University Press

BORGAS, M. S. & SAWFORD, B. L. 1996 Molecular diffusion and viscous effects on concentration statistics in grid turbulence. *J. Fluid Mech.* **324**, 25–54.

CHATWIN, P. C. & SULLIVAN, P. J. 1989 The intermittency factor of scalars in turbulence. *Phys. Fluids* A **1**, 761–763.

CIESZELSKI, R. 1994 Diffusion of pollutants by helical vortices with subgrid turbulence. In *Air Pollution II Vol. I: Computer Simulations* (ed. J. M. Baldasano, C. A. Brebbia, H. Power & P. Zannetti), pp. 175–182. Computational Mechanics Publications, Southampton Boston.

CORRSIN, S. 1951 The decay of isotropic temperature fluctuations in an isotropic turbulence. *J. Aeronaut. Sci.* **18**, 417–423.

DRUMMOND, I. T., DUANE, S. & HORGAN, R. R. 1984 Scalar diffusion in simulated helical turbulence with molecular diffusivity. *J. Fluid Mech.* **138**, 75–91.

ETLING, D. 1985 Some aspects of helicity in atmospheric flows. *Beitr. Phys. Atmos.* **58**, 88–100.

FLESCH, T. K. & WILSON, J. D. 1992 A two-dimensional trajectory-simulation model for non-Gaussian, inhomogeneous turbulence within plant canopies. *Boundary-Layer Met.* **61**, 349–374.

GARDINER, C. W. 1983 *Handbook of Stochastic Methods.* Springer.

INOUE, E. 1952 On the Lagrangian correlation coefficient for turbulent diffusion and application to atmospheric diffusion phenomena. *Geophys. Res. Paper No.* **19**, 397–412.

JAYESH & WARHAFT, Z. 1992 Probability distribution, conditional dissipation, and transport of passive temperature fluctuations in grid-generated turbulence. *Phys. Fluids* A **4**, 2292–2307.

KHOLMYANSKY, M., KIT, E., TEITEL, M. & TSINOBER, A. 1991 Some experimental results on velocity and vorticity measurements in turbulent grid flows with controlled sign of mean helicity. *Fluid Dyn. Res.* **7**, 65–75.

KRAICHNAN, R. H. 1977 Lagrangian velocity covariance in helical turbulence. *J. Fluid Mech.* **81**, 385–398.

MOFFATT, H. K. 1983 Transport effects associated with turbulence, with particular attention to the influence of helicity. *Rep. Prog. Phys.* **46**, 621–664.

MOFFATT, H. K. & TSINOBER, A. 1992 Helicity in laminar and turbulent flow. *Ann. Rev. Fluid Mech.* **24**, 281–312.

OBUKHOV, A. M. 1959 Description of turbulence in terms of Lagrangian variables. *Adv. Geophys.* **6**, 113–115.

POPE, S. B. 1994 Lagrangian PDF methods for turbulent flows. *Ann. Rev. Fluid Mech.* **26**, 23–63.

SAWFORD, B. L. 1991 Reynolds number effects in Lagrangian stochastic models of dispersion. *Phys. Fluids* A **3**, 1577–1586.

SAWFORD, B. L. & BORGAS, M. S. 1994 On the continuity of stochastic models for the Lagrangian velocity in turbulence. *Physica* D **76**, 297–311.

TAYLOR, G. I. 1921 Diffusion by continuous movements. *Proc. Lond. Math. Soc.* **20**, 196–211.

THOMSON, D. J. 1987 Criteria for the selection of stochastic models of particle trajectories in turbulent flows. *J. Fluid Mech.* **180**, 529–556.

ZEMAN, O. 1994 A note on the spectra and decay of rotating homogeneous turbulence. *Phys. Fluids* A **6**, 3221–3223.

https://doi.org/10.1017/S002211209600393X Published online by Cambridge University Press